Chemical and Process Engineering Research
ISSN 2224-7467 (Paper) ISSN 2225-0913 (Online)
Vol.36, 2015

Impact of Thermal Stratification on Unsteady Hiemenz Non-Darcy Copper Nanofluid Flow over a Porous Wedge in the Presence of Magnetic Field Due to Solar Radiation (Green) Energy

R. Kandasamy and I. Muhaimin
Research Centre for Computational Mathematics, FSTPi, Universiti Tun Hussein Onn Malaysia, Malaysia

Abstract
Energy is an important input for economic development. Solar energy is created by light and heat which is emitted by the sun, in the form of electromagnetic radiation. Solar energy is the most readily and abundantly available source of green energy. Copper nanoparticle suspensions in the Cu-water have been proposed as a means to enhance solar collector efficiency through direct absorption of the incoming solar energy. Thermal stratification is the scientific term that describes the layering of bodies of water based copper nanofluid on their temperature. The aim of the present work is to investigate theoretically the effect of thermal stratification in the presence of magnetic field on unsteady Hiemenz non-Darcy flow and heat transfer of incompressible copper nanofluid along a porous wedge due to renewable (solar energy). It is of notable interest in this work to consider the similarity transformation is used for unsteady flow. Copper nanofluid flow past a porous wedge plays a dominant role on absorbs the incident solar radiation and transits it to the working fluid by convection.
Keywords: Nanofluid; Porous wedge; Unsteady non-Darcy flow; Magnetic field; Thermal stratification; Solar energy radiation.

1. Introduction

The radiant heat and light energy from the Sun is called as solar energy. Solar energy is that energy which comes from the natural energy flows on earth. Renewable solar energy is also termed as green energy. The earth receives more energy in just one hour from the sun than what is consumed in the whole world for one year. Initially, the application of nanofluids in collectors and water heaters are investigated from the efficiency, economic, and environmental aspects. Some studies conducted on thermal conductivity and optical properties of nanofluids are also briefly reviewed, because these parameters can determine the capability of nanofluids to enhance the performance of solar systems. Solar collectors are particular kind of heat exchangers that transform solar radiation energy into internal energy of the transport medium.

Nanofluids have been considered for applications as advanced heat transfer fluids for almost two decades. However, due to the wide variety and the complexity of the nanofluid systems, no agreement has been achieved on the magnitude of potential benefits of using nanofluids for heat transfer applications. Nanofluids poses the following advantages as compared to conventional fluids which make them suitable for use in solar energy collectors: Absorption of solar energy will be maximized with change of the size, shape, material and volume fraction of the nanoparticles. The suspended nanoparticles increase the surface area and the heat capacity of the fluid due to the very small particle size. The suspended nanoparticles enhance the thermal conductivity which results improvement in efficiency of heat transfer systems. Properties of fluid can be changed by varying concentration of nanoparticles. The suspension of nano-sized particles (1–100 nm) in a conventional base fluid is called a nanofluid. Choi first used the term “nanofluid” in 1995, Choi (1995).

Saidur et al. (2011) reviewed the potential of nanofluids in the improvement of heat transfer in refrigeration systems. The authors concluded that more studies are required to find the reasons behind the considerable improvements in heat transfer whereas an insignificant increase in pressure occurs. Thomas and Sobhan (2011) presented experimental studies on nanofluids, with emphasis on the techniques of measuring the effective thermal conductivity. Escher et al. (2011) investigated the applications of nanofluids in cooling electronics. Recently, applications of computer simulations and computational fluid dynamics (CFD) used to model systems employing nanofluids were reviewed and analyzed by Abouali and Ahmadi (2012) and Kamyar et al. (2012). Ahn and Kim (2012) also published a review on the critical heat flux of nanofluids for both convective flow boiling and pool boiling applications. In another publication, Saidur et al. (2011)reviewed the general applications of nanofluids in some fields such as cooling of electronics, heat exchangers, medical applications, fuel cells, nuclear reactors, and many more. They also mentioned briefly the applications of nanofluids in solar water heaters. They investigated challenges in using nanofluids, including an increased pressure drop and pumping power, long-term stability of nanoparticles dispersion, and the high cost of nanofluids.

Thermo physical properties of the nanofluids are quite essential to predict their heat transfer behavior. It is extremely important in the control for the industrial and energy saving perspectives. Nanoparticles have

great potential to improve the thermal transport properties compared to conventional particles fluids suspension, millimetre and micrometer sized particles. Radiative transport in porous media has important engineering applications in solar collectors and the porous medium acts as a means to absorb or emit radiant energy that is transferred to or from a fluid. Some previous works are reviewed in which the potential of nanofluids for use in solar energy system is performed through the study of optical properties and thermal conductivity of nanofluids. Link and El-Sayed (2000) reviewed the optical properties of gold nanoparticles. Particularly, they studied the shape and size dependence of radiative, and photo thermal properties of gold nanocrystals. Khlebtsov et al. (2005) investigated the effects of the size, shape, and structure of gold and silver nanoparticles on the optical properties of the nanofluids and perceived that the shape and size of the nanoparticle have great effect on the optical properties of a nanofluid. Sani et al. (2011) reported the optical characterization of a new fluid consisting of single-wall carbon nanohorns and ethylene glycol for solar energy applications. Mercatelli et al. (2011a, 2011b) investigated the potential of single-wall carbon nanohorns nanoparticles with two different base fluids including water and glycol. Mercatelli et al. (2012) applied a simple spectrophotometric to estimate the spectral scattering albedo of water nanofluid. Saidur et al. (2012) investigated the potential of Aluminum/water nanofluid to use in direct absorption solar collectors. Lenert and Wang (2011) and Lenert (2010) presented a combined theoretical and experimental work to optimize the efficiency of liquid-based solar receivers seeded with carbon-coated absorbing nanoparticles. Colangelo et al. (2012) measured the thermal conductivities of CuO, Al_2O_3, ZnO and Cu with different shapes and volume fraction by 3%, where water and diathermic oil are as the base fluids, to evaluate their potential to use for high temperature applications such as in solar collectors. Kameya and Hanamura (2011) found experimentally that the solar radiation absorption for the nanofluid of Ni/alkyl naphthalene with 0.1% volume fraction is much higher than the base fluid. Gan and Qiao (2012a, 2012b) found that for ethanol-based nanofluids, the radiation absorption for nanofluids containing Al_2O_3 nanoparticles is higher than nanofluids containing aluminum nanoparticles. Generally, the fluid itself can be assumed to be transparent to radiation, because the dimensions for radiative transfer among the solid structure elements of the porous medium are usually much less than the radiative mean free path for scattering or absorption in the fluid.

Convective flow in porous media has been widely studied in the recent years due to its wide applications in engineering as post-accidental heat removal in nuclear reactors and solar collectors. The effects of heat transfer laminar boundary layer flow over a wedge have been studied by many authors (Kafoussias and Nanousis (1997), Kandasamy et al. (2008) and Cheng and Lin (2002)) in different situations. Nanofluids are suspensions of nanoparticles in fluids that show significant enhancement of their properties at modest nanoparticle concentration was investigated by Rosmila Abdul-Kahar et al. (2011), Kandasamy et al. (2011), Vajravelu et al. (2011) and Rana and Bhargava (2011). Nanofluids may be used in various applications which include electronic cooling, vehicle cooling transformer and coolant for nuclear reactors. In this paper, we apply the so-called symmetry methods for a particular problem of fluid mechanics. The main advantage of such methods is that they can successfully be applied to non-linear differential equations. The method of Lie group transformations is used to derive all group-invariant similarity solutions of the unsteady two-dimensional laminar boundary-layer equations, Ovsyannikov (1982) and Avramenko et al. (2001). Solar energy is currently one kind of important resource for clean and renewable energy, and is widely investigated in many fields. For this reason, it is of special interest in this work to consider natural convection due to solar radiation non-Darcy flow from a wedge embedded in a porous medium with variable porosity distribution. The inertia effect is expected to be important at a higher flow rate and it can be accounted for through the addition of a velocity squared term in the momentum equation, which is known as the Forchheimer's extension. Several researchers have studied natural convection heat transfer in porous medium by considering Forchheimer's extension. The thermal stratification of nanofluids refers to a change in the temperature at different depths in the nanofluid, and is due to the change in fluid's density with temperature. Nanotechnology is an enabling technology that provides an extensive range of resources to resolve the energy-related problems, as the developing components and appliances are smaller than 100 nm they provide the new ways to catch, store and exchange energy. Every day, the sun shines a huge amount of energy which is generated through a process of nuclear fusion. Even the sun radiates more energy in one second than people have practiced since the beginning of time. It has been noted that the technical potential of solar energy all over the world is many times larger than the current total primary energy demanded.

The effect of magnetic field on natural convection along a wedge plate in a thermally stratified Hiemenz nanofluid flow on non-Darcy porous medium under the convective boundary condition has not been reported in the literature. There is a more common practice situation, where heat transfer occurs at the boundary surface to or from a fluid flowing on the surface at a known temperature and a known heat transfer coefficient, e.g. in heat exchangers, condensers and reboilers. In view of the above said application, the aim of this investigation is to consider the effects of thermal stratification on unsteady Hiemenz non-Darcy copper nanofluid flow over a porous wedge in the presence of magnetic field due to solar radiation (green) energy. Lie symmetry group transformation is utilized to convert the governing partial differential equations into ordinary differential equations and then the numerical solution of the problem is accomplished by using Runge Kutta Gill method

(Gill (1951)) with shooting technique. The effects of magnetic, thermal stratification and convective radiation parameters are examined and are displayed through graphs.

2. Mathematical Analysis

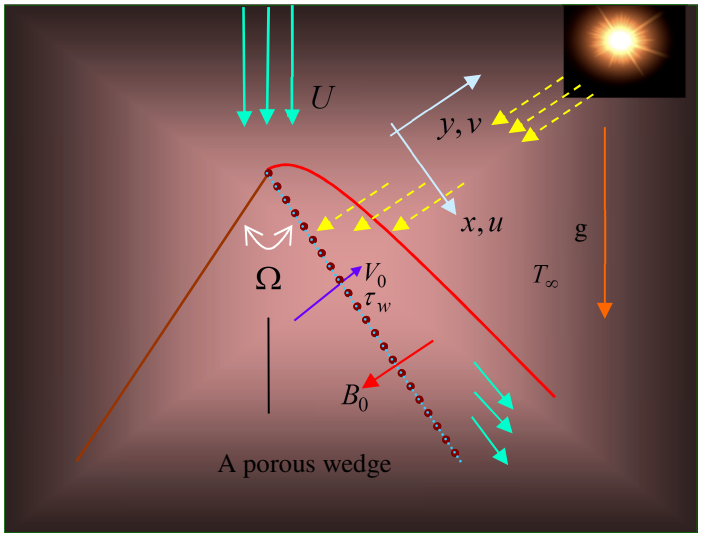

Fig.1 Physical flow model over a porous wedge sheet

Consider the unsteady two-dimensional free convection flow from the wedge flat plate in a thermally stratified, electrically conducting non-Darcy copper nanofluid flow over a porous medium in the presence of solar energy radiation (Fig. 1). Influence of a constant magnetic field of strength B_0 which is applied normally to the sheet and the temperature at the wall of the wedge takes the constant value T_w, whereas the ambient (y tends to infinity), takes the constant value T_∞. The magnetic Reynolds number is assumed to be small so that the induced magnetic field can be neglected. The porous medium is assumed to be transparent and in thermal equilibrium with the fluid. The non reflecting absorbing ideally transparent wedge plate receives an incident radiation flux of intensity q''_{rad} and the porous medium absorbs the incident solar radiation and transits it to the working fluid by convection. This radiation flux penetrates the plate and is absorbed in an adjacent fluid of absorption coefficient. Due to heating of the absorbing nanofluid and the wedge plate by solar radiation, heat is transferred from the plate to the surroundings and the solar radiation is a collimated beam that is normal to the plate and the working fluid is assumed to have heat absorption properties. The thermophysical properties of the nanofluid are given in Kandasamy et al. (2011). Under the above assumptions, the boundary layer equations governing the flow and thermal field can be written in dimensional form as

$$\frac{\partial \bar{u}}{\partial \bar{x}} + \frac{\partial \bar{v}}{\partial \bar{y}} = 0 \tag{1}$$

$$\frac{\partial \bar{u}}{\partial \bar{t}} + \bar{u}\frac{\partial \bar{u}}{\partial \bar{x}} + \bar{v}\frac{\partial \bar{u}}{\partial \bar{y}} = \frac{1}{\rho_{f_n}}\left[\frac{\partial U}{\partial t}\rho_{f_n} + U\frac{dU}{dx}\rho_{f_n} + \mu_{f_n}\frac{\partial^2 \bar{u}}{\partial \bar{y}^2} + (\rho\beta)_{f_n}\bar{g}(T - T_\infty)\sin\frac{\Omega}{2}\right.$$
$$\left. - \frac{F}{\sqrt{K}}\rho_{f_n}(\bar{u}^2 - U^2) - (\sigma B_0^2 + \frac{\nu_f}{K}\rho_{f_n})(\bar{u} - U)\right] \tag{2}$$

$$\frac{\partial T}{\partial \bar{t}} + \bar{u}\frac{\partial T}{\partial \bar{x}} + \bar{v}\frac{\partial T}{\partial \bar{y}} = \alpha_{f_n}\frac{\partial^2 T}{\partial \bar{y}^2} - \frac{1}{(\rho c_p)_{f_n}}\frac{\partial q''_{rad}}{\partial y} + \frac{\mu_{f_n}}{(\rho c_p)_{f_n}}\left(\frac{\partial u}{\partial y}\right)^2 \tag{3}$$

Using Rosseland approximation for radiation (Sparrow and Cess (1978)) we can write $q''_{rad} = -\frac{4\sigma_1}{3k^*}\frac{\partial T^4}{\partial y}$ where σ_1 is the Stefan–Boltzman constant is, k^* is the mean absorption coefficient. The Rosseland approximation is used to describe the radiative heat transfer in the limit of the optically thick fluid (nanofluid).

The boundary conditions of these equations are

$$\bar{u} = 0, \bar{v} = -v_0, T = T_w + c_1 x^{n_1} \ at\ \bar{y} = 0\ ; \bar{u} \to U = \frac{\nu_f\ x^m}{\delta^{m+1}}, T \to T_\infty = (1-n)T_o + n\,T_w\ as\ \bar{y} \to \infty \tag{4}$$

Here c_1 *and* n_1 (power index) are constants and v_0 and T_w are the suction ($v_0 > 0$) or injection ($v_0 < 0$) velocity and the fluid temperature at the plate. The potential flow velocity of the wedge can be written as $U(x,t) = \frac{\nu_f \, x^m}{\delta^{m+1}}$, $\beta_1 = \frac{2m}{1+m}$, m is a constant, whereas δ is the time-dependent length scale which is taken to be as: $\delta = \delta(t)$ and $\beta_1 = \frac{\Omega}{\pi}$ is the Hartree pressure gradient parameter, Ω is the angle of wedge. Here $n = \frac{m_1}{1+m_1}$ (Anjali Devi and Kandasamy (2001)), n refers to thermal stratification parameter, such that $0 \le n < 1$. $\bar{g}$ is the acceleration due to gravity, K is the permeability of the porous medium, F is the empirical constant in the second-order resistance and setting $F = 0$ in Equ. (2) is reduced to the Darcy law. v_o is the velocity of suction / injection, ρ_{f_n} is the effective density of the nanofluid, μ_{f_n} is the effective dynamic viscosity of the nanofluid, α_{f_n} is the thermal diffusivity of the nanofluid which are defined as (see Aminossadati and Ghasemi (2009)),

$$\rho_{f_n} = (1-\zeta)\rho_f + \zeta\rho_s, \quad \mu_{f_n} = \frac{\mu_f}{(1-\zeta)^{2.5}}; (\rho\beta)_{f_n} = (1-\zeta)(\rho\beta)_f + \zeta(\rho\beta)_s, \quad \alpha_{f_n} = \frac{k_{f_n}}{(\rho\, c_p)_{f_n}},$$

$$(\rho\, c_p)_{f_n} = (1-\zeta)(\rho\, c_p)_f + \zeta(\rho\, c_p)_s \quad \frac{k_{f_n}}{k_f} = \left\{\frac{(k_s + 2k_f) - 2\zeta(k_f - k_s)}{(k_s + 2k_f) + 2\zeta(k_f - k_s)}\right\}, \text{(Maxwell (1891))} \qquad (5)$$

It represents the lower limit for the thermal conductivity of nanofluids and it can seen that in the limit where ζ = 0 (no particles), Equ. (5) yields $k_{low} = 1$ as expected. Experiments report thermal conductivity enhancement of nanofluids be yond the Maxwell limit of 3ζ. In the limit of low particle volume concentration (ζ) and the particle conductivity (k_s), being much higher than the base liquid conductivity (k_f), Equ. (5) can be reduced to Maxwell 3ζ limit as:

$$k_{low} = \frac{k_{f_n}}{k_f} = 1 + 3\zeta \qquad (6)$$

μ_f is the dynamic viscosity of the base fluid, β_f and β_s are the thermal expansion coefficients of the base fluid and nanoparticle, respectively, ρ_f and ρ_s are the density of the base fluid and nanoparticle, respectively, k_{f_n} is the effective thermal conductivity of the nanofluid and $(\rho\, c_p)_{f_n}$ is the heat capacitance of the nanofluid. By introducing the following non-dimensional variables

$$x = \frac{\bar{x}}{\sqrt{\frac{\nu_f}{c}}}, y = \frac{\bar{y}}{\sqrt{\frac{\nu_f}{c}}}, u = \frac{\bar{u}}{\sqrt{c\nu_f}}, v = \frac{\bar{v}}{\sqrt{c\nu_f}} \; and \; \theta = \frac{T - T_\infty}{T_w - T_\infty} \qquad (7)$$

Equations (1)-(4) take the non-dimensional form

$$\frac{\partial u}{\partial x} + \frac{\partial v}{\partial y} = 0 \qquad (8)$$

$$\frac{\partial u}{\partial t} + u\frac{\partial u}{\partial x} + v\frac{\partial u}{\partial y} = \frac{1}{(1-\zeta+\zeta\frac{\rho_s}{\rho_f})}[\{\frac{\partial U}{\partial t} + U\frac{dU}{dx} - \frac{F}{\sqrt{K}}(u^2 - U^2)\}\frac{\rho_{f_n}}{\rho_f} + \frac{\nu_f}{(1-\zeta)^{2.5}}\frac{\partial^2 u}{\partial y^2}$$

$$+\{(1-\zeta+\zeta\frac{(\rho\beta)_s}{(\rho\beta)_f})\gamma\sin\frac{\Omega}{2}\theta\} - (\frac{\sigma B_0{}^2}{\rho_f} + \frac{\nu_f}{K(1-\zeta)^{2.5}})(u-U)] \qquad (9)$$

$$\frac{\partial T}{\partial t} + u\frac{\partial T}{\partial x} + v\frac{\partial T}{\partial y} = \frac{1}{1-\zeta+\zeta\frac{(\rho\, c_p)_s}{(\rho\, c_p)_f}}[\frac{1}{\mathrm{Pr}_f}\{\frac{k_{f_n}}{k_f}\frac{\partial^2 T}{\partial y^2} + \frac{4}{3}N\left((C_T+\theta)^3\theta'\right)' + \frac{\mu_{f_n}}{(\rho\, c_p)_f}\left(\frac{\partial u}{\partial y}\right)^2\}] \qquad (10)$$

with the boundary conditions

$$\bar{u} = 0, \bar{v} = -V_0, T = T_w \; at \; \bar{y} = 0; \bar{u} \to U = \frac{\nu_f \, x^m}{\delta^{m+1}}, T \to T_\infty = (1-n)T_o + nT_w \; as \; \bar{y} \to \infty \qquad (11)$$

Prandtl number $\Pr_f = \frac{\nu_f}{\alpha_f}$, porous media parameter $\lambda = \frac{\delta^{m+1}}{K\,k^2}$, buoyancy or natural convection parameter $\gamma = \frac{g\,(\rho\beta)_f \Delta T}{\rho_f\, U^2\, k^{\frac{2}{1-m}}}$,conductive radiation parameter $N = \frac{4\sigma_1 \theta_w^3}{k_f\, k^*}$, Forchheimer number $F_n = \left(\frac{\xi}{k}\right)^{\frac{2}{1-m}} \frac{F}{\sqrt{K}}$, Eckert number $Ec = \frac{\mu_f}{(\rho\, c_p)_f} \frac{U^2}{(T_w - T_\infty)}$, magnetic parameter $M = \frac{\sigma\, B_0{}^2}{\mu_f} \frac{\delta^{m+1}}{k^2}$ and $C_T = \frac{T_\infty}{T_w - T_\infty}$ is the temperature ratio where C_T assumes very small values by its definition as $T_w - T_\infty$ is very large compared to T_∞ and it is assigned the value 0.1. It is worth mentioning that $\gamma > 0$ aids the flow and $\gamma < 0$ opposes the flow, while $\gamma = 0$ i.e., $(T_w - T_\infty)$ represents the case of forced convection flow. On the other hand, if γ is of a significantly greater order of magnitude than one, then the buoyancy forces will be predominant. Hence, combined convective flow exists when $\gamma = O(1)$.

Following the lines of Kafoussias and Nanousis (1997), the changes of variables are

$$\eta = y\sqrt{\frac{(1+m)}{2}}\sqrt{\frac{x^{m-1}}{\delta^{m+1}}}\,,\psi = \sqrt{\frac{2}{1+m}}\frac{\nu_f\, x^{\frac{m+1}{2}}}{\delta^{\frac{m+1}{2}}} f(\eta) \text{ and } \theta = \frac{T - T_\infty}{T_w - T_\infty} \tag{12}$$

By introducing the stream function ψ, which defined as $u = \frac{\partial \psi}{\partial y}$ and $v = -\frac{\partial \psi}{\partial x}$, then the system of equations (8) - (10) become

$$\frac{\partial^2\psi}{\partial t\partial y} + \frac{\partial\psi}{\partial y}\frac{\partial^2\psi}{\partial x\partial y} - \frac{\partial\psi}{\partial x}\frac{\partial^2\psi}{\partial y^2} = \frac{1}{(1-\zeta+\zeta\frac{\rho_s}{\rho_f})}[\{(1-\zeta+\zeta\frac{(\rho\beta)_s}{(\rho\beta)_f})\,\gamma\sin\frac{\Omega}{2}\theta\} + \frac{1}{(1-\zeta)^{2.5}}\frac{\partial^3\psi}{\partial y^3}$$
$$+\{\frac{\partial U}{\partial t} + U\frac{dU}{dx} - \frac{F}{\sqrt{K}}((\frac{\partial\psi}{\partial y})^2 - U^2)\}\frac{\rho_{f_n}}{\rho_f} - (\frac{\sigma B_0{}^2}{\rho_f} + \frac{\nu_f}{K(1-\zeta)^{2.5}})(\frac{\partial\psi}{\partial y} - U)] \tag{13}$$

$$\frac{\partial\theta}{\partial t} + \frac{\partial\psi}{\partial y}\frac{\partial\theta}{\partial x} - \frac{\partial\psi}{\partial x}\frac{\partial\theta}{\partial y} = \frac{1}{1-\zeta+\zeta\frac{(\rho\,c_p)_s}{(\rho\,c_p)_f}}[\frac{1}{\Pr_f}\{\frac{k_{f_n}}{k_f}\frac{\partial^2\theta}{\partial y^2}$$
$$+\frac{4}{3}N\left((C_T+\theta)^3\theta'\right)' + \frac{\mu_{f_n}}{(\rho\,c_p)_f}\left(\frac{\partial^2\psi}{\partial y^2}\right)^2\}] \tag{14}$$

with the boundary conditions

$$\bar{u} = 0, \bar{v} = -V_0, T = T_w \text{ at } \bar{y} = 0\,; \bar{u} \to U = \frac{\nu_f\, x^m}{\delta^{m+1}}, T \to T_\infty = (1-n)T_o + n\,T_w \text{ as } \bar{y} \to \infty \tag{15}$$

The symmetry groups of Equs. (13) and (14) are calculated using classical Lie group approach, Kandasamy et al. (2011) as

$$f''' - \frac{\frac{2}{m+1}(1-\zeta)^{2.5}\xi^2}{(1-\zeta+\zeta\frac{\rho_s}{\rho_f})}[(M+\frac{\lambda}{(1-\zeta)^{2.5}})(f'-1) - \xi^{\frac{1}{1-m}}\{(1-\zeta+\zeta\frac{(\rho c_p)_s}{(\rho c_p)_f})\}\gamma\sin\frac{\Omega}{2}\theta]$$

$$-(1-\zeta+\zeta\frac{\rho_s}{\rho_f})(1-\zeta)^{2.5}[\frac{2}{m+1}(m-F_n)(f'^2-1) - f\,f'' + \lambda_u(2-\eta\,f'' - 2f') + \frac{1-m}{1=m}\xi\frac{\partial f}{\partial\xi}(\frac{\partial f}{\partial\eta} - \frac{\partial^2 f}{\partial\eta^2})] = 0 \tag{16}$$

$$\theta'' + \frac{4}{3}\frac{k_f}{k_{f_n}} N\{(C_T+\theta)^3\theta'\}' + \frac{\mathrm{Pr}_f}{(1-\zeta)^{2.5}} Ec\,(f'')^2 - \mathrm{Pr}_f\{1-\zeta+\zeta\frac{(\rho c_p)_s}{(\rho c_p)_f}\}\times$$
$$\frac{k_f}{k_{f_n}}[\frac{2n_1}{m+1} f'\left(\theta+\frac{n}{1-n}\right) - f\theta' + \lambda_v\eta\,\theta' + \frac{1-m}{1+m}\{\xi\frac{\partial\theta}{\partial\xi}\frac{\partial f}{\partial\eta} - \xi\frac{\partial f}{\partial\xi}\frac{\partial\theta}{\partial\eta}\}] = 0 \quad (17)$$

The boundary conditions take the following form

$$\frac{\partial f}{\partial\eta} = 0, \frac{m+1}{2} f + \frac{1-m}{2}\xi\frac{\partial f}{\partial\xi} = -S, \theta = 1 \; at \; \eta = 0 \; and \; \frac{\partial f}{\partial\eta} = 1, \theta \to 0 \; as \; \eta \to \infty \quad (18)$$

S is the suction parameter if $S>0$ and injection if $S<0$ and $\xi = k\,x^{\frac{1-m}{2}}$ Kafoussias and Nanousis (1997), is the dimensionless distance along the wedge ($\xi>0$). In this system of equations, it is obvious that the nonsimilarity aspects of the problem are embodied in the terms containing partial derivatives with respect to ξ. At the first level of truncation, the terms accompanied by $\xi\frac{\partial}{\partial\xi}$ are small. This is particularly true when ($\xi<<1$). Thus the terms with $\xi\frac{\partial}{\partial\xi}$ on the right-hand sides of Equations (20) and (21) are deleted to get the following system of equations:

$$f''' - \frac{\frac{2}{m+1}(1-\zeta)^{2.5}\xi^2}{(1-\zeta+\zeta\frac{\rho_s}{\rho_f})}[(M+\frac{\lambda}{(1-\zeta)^{2.5}})(f'-1) - \xi^{\frac{1}{1-m}}\{(1-\zeta+\zeta\frac{(\rho c_p)_s}{(\rho c_p)_f})\}\gamma\sin\frac{\Omega}{2}\theta]$$
$$-(1-\zeta+\zeta\frac{\rho_s}{\rho_f})(1-\zeta)^{2.5}[\frac{2}{m+1}(m-F_n)(f'^2-1) - f\,f'' + \lambda_u(2-\eta f'' - 2f')] = 0 \quad (19)$$

$$\theta'' + \frac{4}{3}\frac{k_f}{k_{f_n}} N\{(C_T+\theta)^3\theta'\}' + \frac{\mathrm{Pr}_f}{(1-\zeta)^{2.5}} Ec\,(f'')^2$$
$$-\mathrm{Pr}_f\{1-\zeta+\zeta\frac{(\rho c_p)_s}{(\rho c_p)_f}\}\frac{k_f}{k_{f_n}}[\frac{2n_1}{m+1} f'\left(\theta+\frac{n}{1-n}\right) - f\theta' + \lambda_v\eta\,\theta'] = 0 \quad (20)$$

The boundary conditions take the following form

$$f' = 0, f = -\frac{2S}{m+1}, \theta = 1 \; at \; \eta = 0 \; and \; f' = 1, \theta \to 0 \; as \; \eta \to \infty \quad (21)$$

Further, we suppose that $\lambda_v = \frac{c}{x^{m-1}}$ where c is a constant so that $c = \frac{\delta^m}{\nu_f}\frac{d\delta}{dt}$ and integrating, it is obtained that $\delta = \left[c(m+1)\nu_f\, t\right]^{\frac{1}{m+1}}$.When $c=2$ and $m=1$ in δ and we get $\delta = 2\sqrt{\nu_f\, t}$ which shows that the parameter δ can be compared with the well established scaling parameter for the unsteady boundary layer problems (see Schlichting (1979)). The functions $f(\eta)$ and $\theta(\eta)$ allow us to determine the skin friction coefficient and Nusselt number as

$$C_f = \frac{\mu_{f_n}}{\rho_f U^2}\left(\frac{\partial u}{\partial y}\right)_{at\; y=0} = -\frac{1}{(1-\zeta)^{2.5}}(\mathrm{Re}\,x)^{-\frac{1}{2}} f''(0) \quad (22)$$

$$Nu_x = \frac{x k_{f_n}}{k_f(T_w - T_\infty)}\left(\frac{\partial T}{\partial y}\right)_{at\; y=0} = -(\mathrm{Re}\,x)^{\frac{1}{2}}\frac{k_{f_n}}{k_f}\theta'(0)\left[1+\frac{4}{3}N(C_T+\theta(0))^3\right] \quad (23)$$

respectively. Here, $\mathrm{Re}_x = \frac{U\,x}{\nu_f}$ is the local Reynolds number.

3. Numerical Analysis

Equations (19) and (20) under the boundary conditions (21) are solved numerically by applying Runge–Kutta-Gill (Gill (1951)) integration scheme together with shooting iteration technique with $\mathrm{Pr}_f, \zeta, \lambda, n_1, \lambda_v$

S, Ω, M, F_n *and* N as prescribed parameters. The details of the solution method are omitted here to conserve space. In the numerical solution, a check was made to confirm that smoothness conditions at each of the boundary layers were satisfied and also the step size of $\Delta\eta = 0.001$ was selected to be satisfactory for a convergence criterion of 10^{-6} in all cases. The case $\gamma >> 1.0$ corresponds to pure free convection, $\gamma = 1.0$ corresponds to mixed convection and $\gamma << 1.0$ corresponds to pure forced convection. Throughout this calculation we have considered $\gamma = 2.0$ unless otherwise specified.

4. Results and Discussion

In order to validate our method, we have compared the results of $f(\eta), f'(\eta)$ *and* $f''(\eta)$ for various values of η (Table.1) with those of White (2006) and the results are found to be in very good agreement. The velocity and temperature profiles for different values of ξ are compared with the available exact solution of Minkowycz and Sparrow (1988) is shown in Fig.2. It is observed that the agreement with the theoretical solution of velocity profile is excellent.

Table 1: Comparison of the current results with previous published work

η	White (2006)			Present works		
0.0	0.000000	0.000000	0.469599	0.000000	0.000000	0.469686
1.0	0.23299	0.46063	0.43438	0.232986	0.460628	0.434377
2.0	0.88680	0.81669	0.25567	0.886797	0.816687	0.255668
3.0	1.79557	0.96905	0.06771	1.795569	0.969046	0.067714

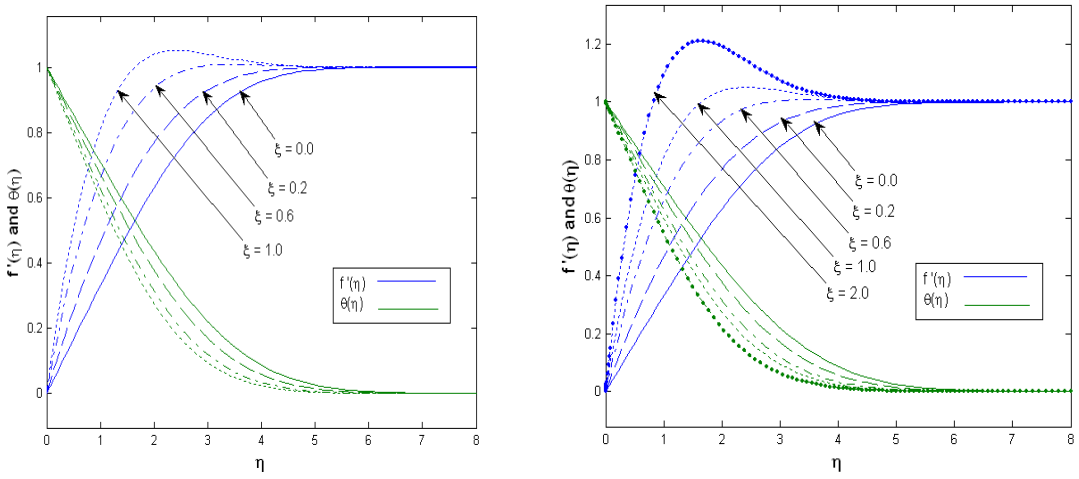

Minkowycz and Sparrow (1988), Present work

Fig.2: Comparison of the velocity and temperature profiles with Minkowycz and Sparrow (1988)

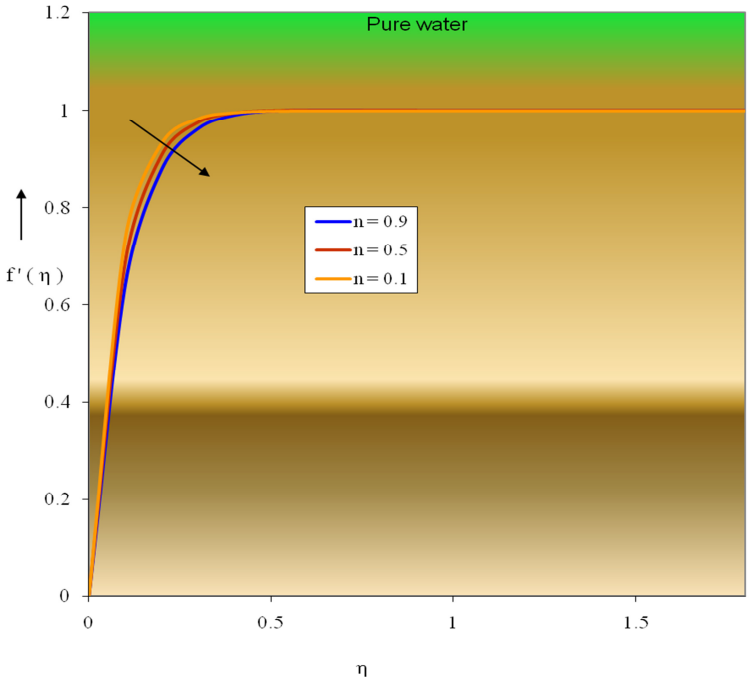

Fig.3 Velocity profiles for various values of thermal stratification $\zeta = 0.05, N = 0.5, M = 1.0$ *and* $m = 0.0909(\Omega = 30^0)$ *– Pure water*

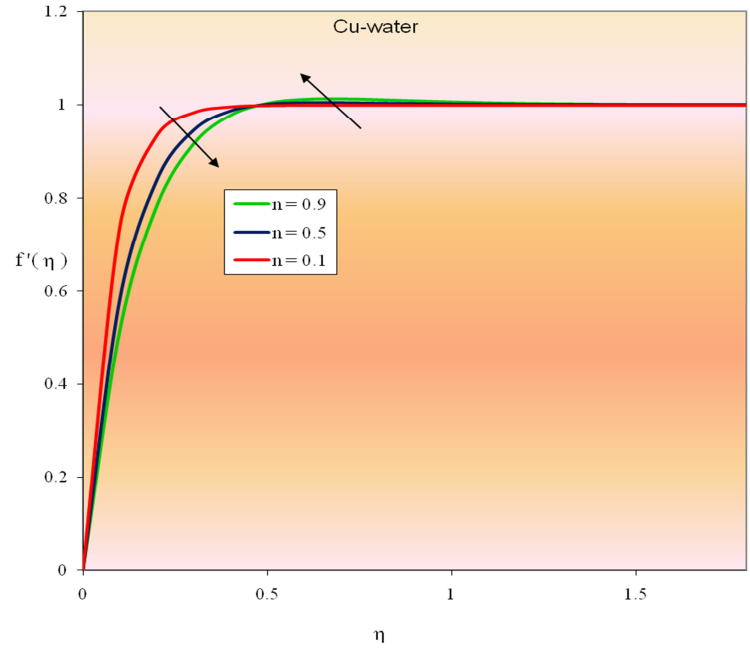

Fig.4 Velocity profiles for various values of thermal stratification $\zeta = 0.05, N = 0.5, M = 1.0$ *and* $m = 0.0909(\Omega = 30^0)$ *– Cu – water*

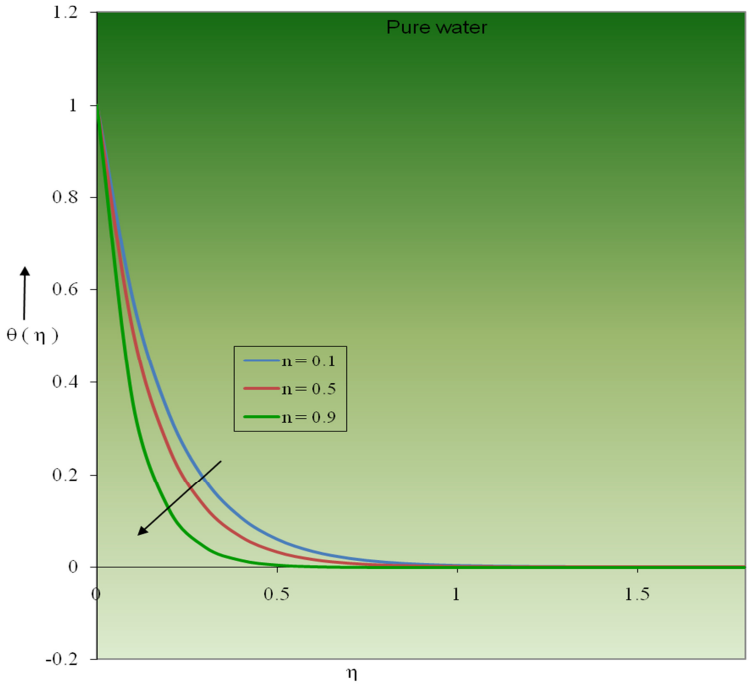

Fig.5 Temperature profiles for various values of thermal stratification $\zeta = 0.05, N = 0.5, n = 0.6$ *and* $m = 0.0909(\Omega = 30^0)$ *– Pure water*

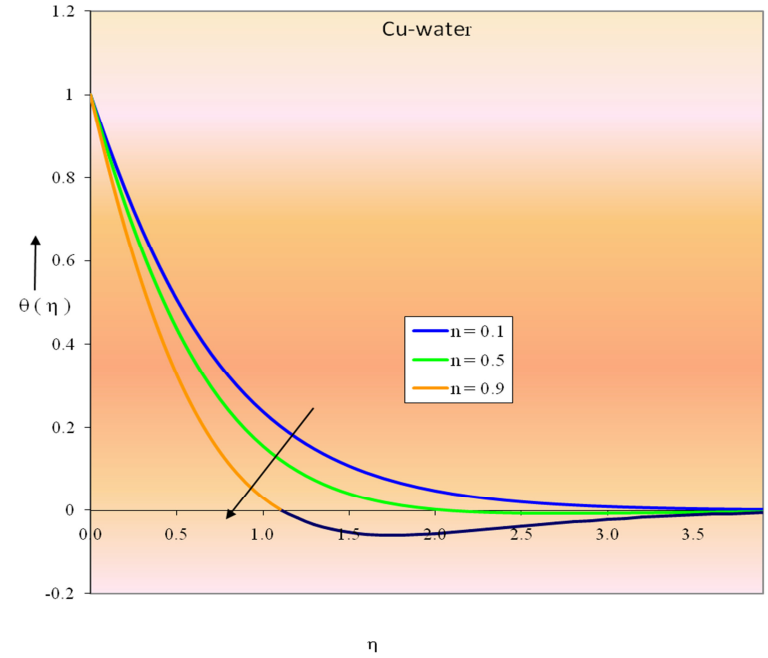

Fig.6 Temperature profiles for various values of thermal stratification $\zeta = 0.05, N = 0.5, n = 0.6$ *and* $m = 0.0909(\Omega = 30^0)$ *– Cu – water*

Figs. 3-6 represent typical velocity and temperature profiles for different values of thermal stratification parameter in the presence of base fluid (pure water) and nanofluid (Cu-water). In the presence of base fluid (Figs. 3 and 5) and copper nanofluid ((Figs. 4 and 6), it is observed that the velocity and temperature decelerate with increase of the strength of thermal stratification, n. Particularly, it is shown that the velocity profiles in the case of copper nanofluid decreases when $\eta \le 0.5$ whereas it increases when $\eta > 0.5$ because

of the dynamic thermal conductivity and viscosity are not only dependent on volume fraction of copper nanoparticle, also highly dependent on other parameters such as particle shape, size, mixture combinations and slip mechanisms, surfactant, etc. For hydrodynamic characteristics mechanism, it is interesting to note from Fig. 4 that the positive value of the velocity profile is observed in the outer boundary region for $n \le 0.1$ (see Fig. 4) since the copper nanofluid has noticeable higher thermal conductivities than the base fluid. It is seen that as thermal stratification parameter increases the thermal boundary layer thickness decreases. This is due to the fact that the thermal stratification parameter n is directly proportional to the heat transfer coefficient and the dynamic viscosity of the nanofluid. On the other hand it is interesting to note that the negative value of the temperature profile is predicted in the outer boundary region for $n = 0.9$. It is concluded that the addition of nanoparticles showed an improvement in the heat transfer rate from the surface. Therefore, the type of copper nanofluid is a key factor for heat transfer enhancement. The thermal stratification is based on a natural process: since warm water is lighter than cold water, it will ascend until it reaches a layer of warmer water or the top of the tank. This process facilitates the efficient utilization of solar heat: The higher the temperature difference between collector and solar storage and the longer such a difference exists, the higher the efficiency of solar heating. The principle of thermal stratification in insulation of the storage tank is of very high importance to the efficiency of a solar heating system. Thermal stratification in storage tanks for solar domestic hot water is essential to improve the efficiency of solar collectors and deliver more useful energy on demand. Thermal stratification and water temperature dynamics have profound effects in chemical and biological reservoir processes. Suspensions of copper nanoparticles in base fluid (Cu-nanofluid) show remarkable thermal and optical property changes from the base fluid at low particle loadings.

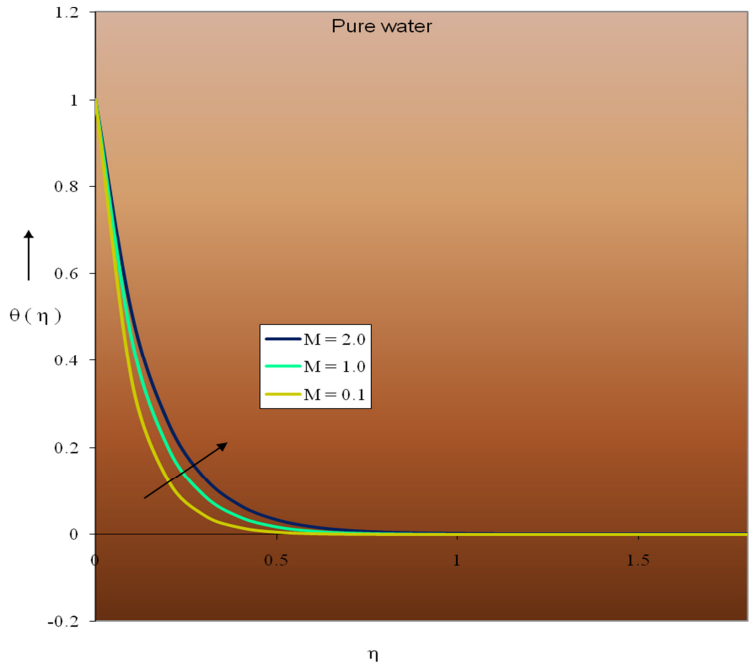

Fig.7 Temperature profiles for various values of magnetic parameter $\zeta = 0.05, N = 0.5, n = 0.6$ *and* $m = 0.0909(\Omega = 30^0)$ *– Pure water*

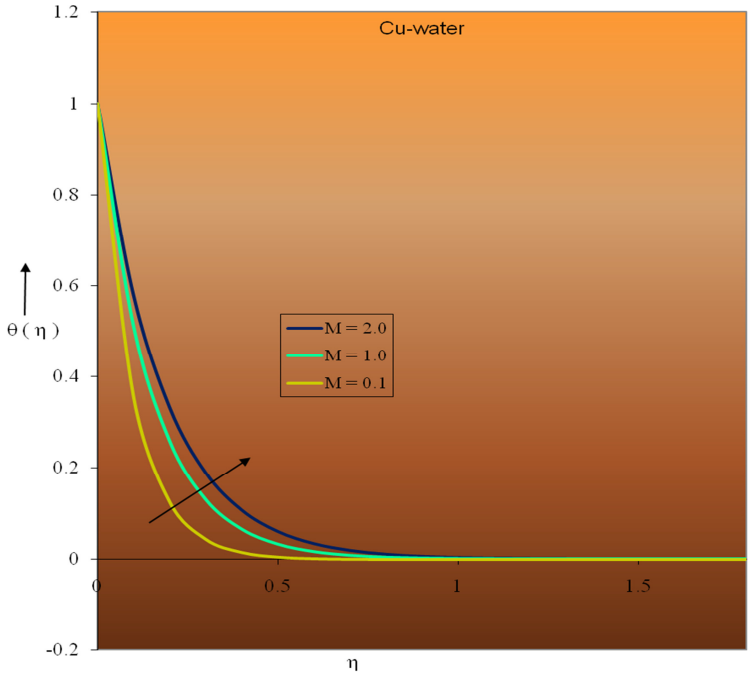

Fig.8 Temperature profiles for various values of magnetic parameter $-\zeta = 0.05, N = 0.5, n = 0.6$ *and* $m = 0.0909(\Omega = 30^0) - Cu - water$

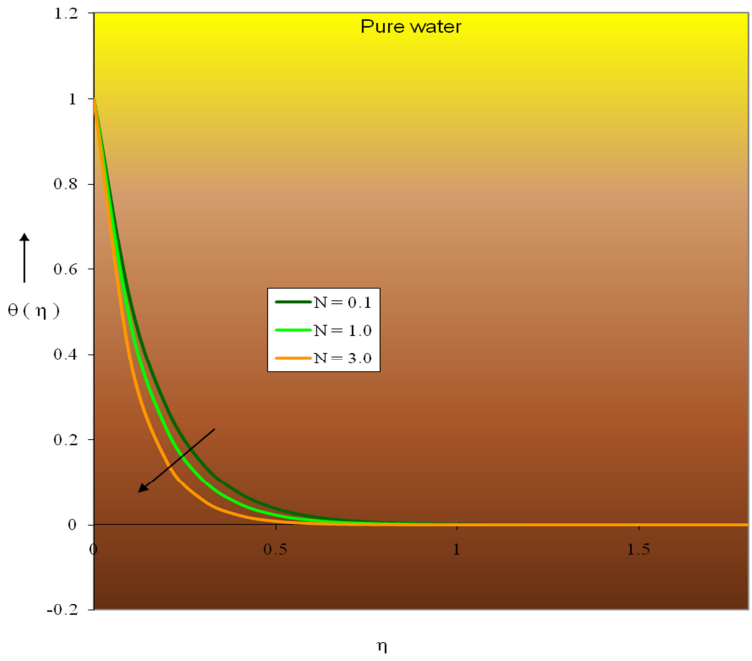

Fig.9 Temperature profiles for various values of thermal radiation $\zeta = 0.05, n = 0.5, M = 1.0$ *and* $m = 0.0909(\Omega = 30^0) - Pure\ water$

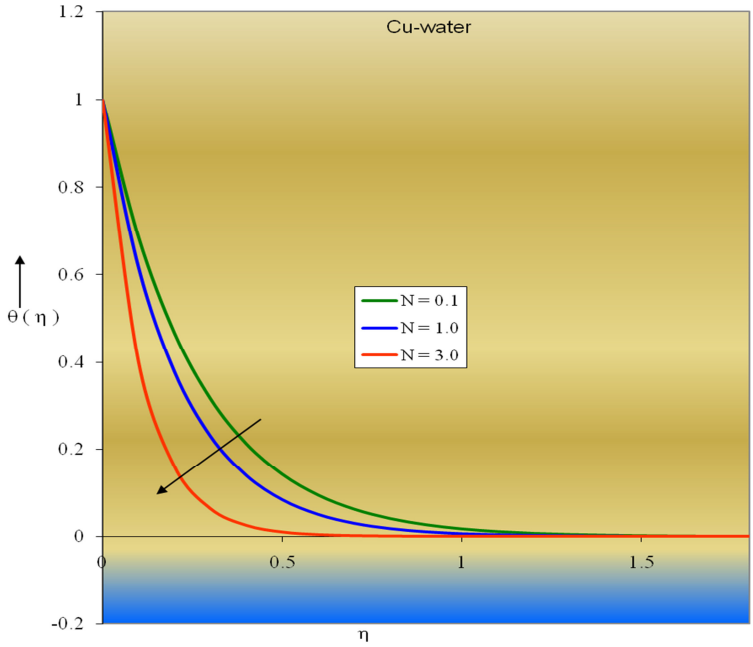

Fig.10 *Temperature profiles for* var*ious values of thermal radiation* $\zeta = 0.05, n = 0.5, M = 1.0$ *and* $m = 0.0909(\Omega = 30^0) - Cu - water$

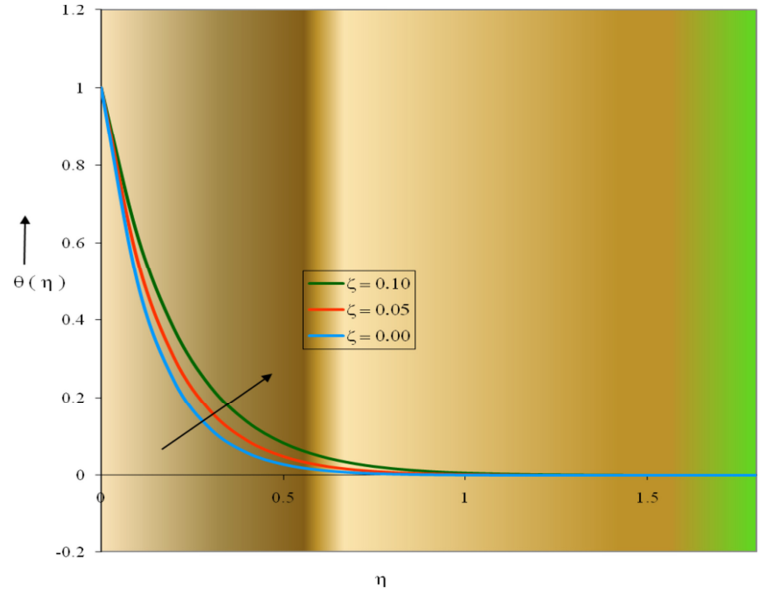

Fig.11 *Temperature profiles for* var*ious values of nanoparticlev volume fraction* $n = 0.5, N = 0.5, M = 1.0$ *and* $m = 0.0909(\Omega = 30^0)$

The nondimensional temperature $\theta(\eta)$ for various values of magnetic parameter in the presence of base fluid and Cu-water are shown in Figs. 7 and 8. In both the cases, the temperature enhances with the increase of magnetic parameter. The magnetic field opposes the transport process. Actually, the increase of M leads to the increase of the Lorentz force arising because of interaction of magnetic and electric fields for the motion of an electrically conducting fluid, and the stronger Lorentz force produces much more resistance to the transport phenomena and it has the tendency to increase the temperature in nanofluid motion. Consequently, the thermal boundary layer thickness becomes thicker for stronger magnetic field. In all cases, the temperature vanishes at

some large distance from the surface of the wedge. This result qualitatively agrees with the expectations, since magnetic field exerts retarding force on the natural convection flow. Physically, it is interesting to note that the temperature of the nanofluid (Cu Water) increases significantly as compared to that of the base fluid because the copper nanofluid has high thermal conductivity. Magnetic copper nanoparticles in nanofluid is a unique material that has both the liquid and magnetic properties. Many of the physical properties of these fluids can be tuned by varying magnetic field. These results clearly demonstrate that the magnetic field can be used as a means of controlling the flow and heat transfer characteristics.

Thermal radiation is one of the principal mechanisms of heat transfer. Temperature profiles for different values of the thermal radiation parameter N in the presence of base fluid (pure water) and nanofluid (Cu-water) are shown in Figs. 9 and 10. In the presence of (pure water) and nanofluid (Cu-water), it is observed that the temperature reduces with increase of the radiation parameter N . The effect of radiation is to decrease the rate of energy transport to the fluid, thereby decreasing the temperature of the fluid. This is because the large values correspond to an increased dominance of conduction over radiation thereby decreasing buoyancy force and thickness of the thermal boundary layer, despite of improved thermal conductivity for specific volume concentration of copper nanoparticles. It is interesting to note that the temperature of the Cu-nanofluid is decelerated significantly as compared to that of the base fluid with increase of thermal radiation because of thermal conductivity of the copper nanofluid. It should be noted that the enhancement of heat transfer greatly depends on particle type, particle size, base fluid, flow regime and specially boundary condition. This is in agreement with the physical fact that the thermal boundary layer thickness decreases with increasing radiation parameter N. Nanofluid-based direct solar collectors are solar thermal collectors where nanoparticles in a liquid medium can scatter and absorb solar radiation. They have recently received interest to efficiently distribute solar energy. Nanofluids have recently found relevance in applications requiring quick and effective heat transfer such as industrial applications, cooling of microchips, microscopic fluidic applications, etc. Nanoparticle materials including copper have been added to different base fluids and characterized in terms of their performance for improving heat transfer efficiency.

Fig. 11 illustrates the effect of nanoparticle volume fraction ζ on temperature profile. It is clear that the temperature of the nanofluid increases with increase of nanoparticle volume fraction and tends asymptotically to zero as the distance increases from the boundary. It is also observed that the temperature distribution in Silver–water and Alumina-water nanofluids are higher than that of Cu–water nanofluid. It is observed that with increasing ζ , the thermal boundary layer thickness increases. This agrees with the physical behavior, when the volume of nanoparticles increases the thermal conductivity and then the thermal boundary layer thickness increases. The variation of the Prandtl number within the boundary layer for different values of the unsteadiness parameter λ_v plays a dominant role on nanofluid flow field. Significant change in the rate of decrease of θ for increasing values of λ_v is noticed. Temperature at a point on the sheet decreases significantly with the increase in λ_v i.e. rate of heat transfer increases with increasing unsteadiness parameter λ_v . Non-Darcy behavior is important for describing nanofluid flow in porous media in situations where high velocity occurs. This is consistent with the fact that non-Darcy behavior is more severe in low permeability porous media. All these physical behavior are due to the combined effects of the strength of volume fraction of the nanoparticles in the presence of non-Darcy flow. The nanoparticles suspension demonstrates some unique and novel thermal properties when compared to the traditional heat transfer of fluids.

5. Conclusions

In the present work, the effect of thermal stratification on MHD unsteady non-Darcy flow and heat transfer of incompressible copper nanofluid past a porous wedge due to solar energy have been analyzed. It is of notable interest in this work to consider the similarity transformation is used for unsteady flow.

1 In the presence of base fluid and copper nanofluid flow, it is seen that the velocity and temperature decelerate with increase of the strength of thermal stratification. In the case of copper nanofluid, it is interesting to note that the positive value of the velocity and negative value of the temperature profiles are observed in the outer boundary region which is due to the layering effect of thermal stratification as it acts like a resistive force.

2 Physically, it is interesting to note that the temperature of the copper nanofluid increases significantly as compared to that of the base fluid with increase of magnetic field because of the transport properties of copper nanofluid. Copper nanoparticles in the magnetic field are a unique material that has both the nanofluid and magnetic properties.

3 It is noticed that the temperature of the copper nanofluid is decelerated significantly as compared to that of the base fluid with increase of convective radiation because the effect of solar radiation is to decrease the rate of energy transport to the copper nanofluid.

5 Increase of thermal boundary layer field due to increase in nanoparticle volume fraction parameter shows that the temperature decreases gradually as we replace Copper nanofluid, $\zeta = 0.05$ by Silver, $\zeta = 0.10$ and Alumina nanofluid, $\zeta = 0.15$ in the said sequence. It implies that the thermal conductivity of nanofluid is strongly dependent on the nanoparticle volume fraction. Hiemenz copper nanofluid flow over a porous wedge plays a significant role on absorbs the incident solar radiation and transits it to the working fluid by convection.

Recently, the dynamics of thermally stratified fluid has attracted attention of researchers and emerged as an important topic for scientific enquiry because of its wide applications in a number of industrial, engineering and environmental applications. Nanofluids due to solar energy are important because they can be used in numerous applications involving heat transfer and other applications such as in detergency, solar collectors, drying processes, heat exchangers, geothermal and oil recovery, building construction, etc. Convective heat transfer coefficient of nanofluids is higher than those of the base fluid. The increases in effective thermal conductivity are important in improving the heat transfer behavior of fluids. The determination of nanofluid thermophysical properties is an increasingly important area in nanofluid cooling applications.

References

Abouali, O., Ahmadi, G., 2012. Computer simulations of natural convection of single phase nanofluids in simple enclosures: a critical review, Appl. Therm. Eng. 36, 1–13.

Ahn, H.S., Kim, M.H., 2012. A review on critical heat flux enhancement with nanofluids and surface modification. ASME J. Heat Transfer. 134, 024001-1-13.

Aminossadati, A.M., Ghasemi, B., 2009. Natural convection cooling of a localized heat source at the bottom of a nanofluid-filled enclosure. Eur. J. Mech. B/Fluids. 28, 630-640.

Anjali Devi, S.P., Kandasamy, R., 2001. Thermal stratification effects on laminar boundary-layer flow over a wedge with suction or injection, Mechanics Research Communications, 28, 349-354.

Avramenko, A.A., Kobzar, S.G., Shevchuk, I.V., Kuznetsov, A.V., Iwanisov, L.T., 2001. Symmetry of turbulent boundary layer flows: investigation of different Eddy viscosity models, Acta Mech., 151, 1-14.

Cheng, W.T., Lin, H.T., 2002. Non-similarity solution and correlation of transient heat transfer in laminar boundary layer flow over a wedge. Int. J. of Engg. Science. 40, 531-540.

Choi, U.S., 1995. Enhancing thermal conductivity of fluids with nanoparticles. ASME FED.231, 99–103.

Colangelo, G., Favale, E., De Risi, A., Laforgia, D., 2012. Results of experimental investigations on the heat conductivity of nanofluids based on diathermic oil for high temperature applications. Appl. Energy. 97, 828–833.

Escher, W., Brunschwiler, T., Shalkevich, N., Shalkevich, A., Burgi, T., Michel, B., Poulikakos, D., 2011. On the cooling of electronics with nanofluids.ASME J. Heat Transfer. 133, 051401-1-11.

Gan, Y., Qiao, L., 2012a. Optical properties and radiation-enhanced evaporation of nanofluid fuels containing carbon-based nanostructures. Energy Fuels. 26, 4224–4230.

Gan, Y., Qiao, L., 2012b. Radiation-enhanced evaporation of ethanol fuel containing suspended metal nanoparticles. Int. J. Heat Mass Transfer. 55, 5777–5782.

Gill, S., 1951. A process for the Step-by-Step Integration of Differential Equations in an Automatic
Digital Computing Machine. Proceedings of the Cambridge Philo. Society. 47, 96-108.

Kamyar, A., Saidur, R., Hasanuzzaman, M., 2012. Application of computational fluid dynamics (CFD) for nanofluids. Int. J. Heat Mass Transfer. 55, 4104-4115.

Kandasamy, R., Muhaimin, I., Ishak Hashim, Ruhaila, 2008. Thermophoresis and chemical reaction effects on non-Darcy mixed convective heat and mass transfer past a porous wedge with variable viscosity in the presence of suction or injection. Nuclear Engg. and Design. 238, 2699-2705.

Kandasamy, R., Loganathan, P., Puvi Arasu, P., Scaling group transformation for MHD boundary- layer flow of a nanofluid past a vertical stretching surface in the presence of suction / injection. Nuclear Engg. and Design. 241, 2053-2059.

Kameya, Y., Hanamura, K., 2011. Enhancement of solar radiation absorption using nanoparticle suspension. Solar Energy. 85, 299–307.

Kafoussias, N.G., Nanousis, N.D., 1997. Magnetohydrodynamic laminar boundary layer flow over a wedge with suction or injection. Canadian Journal of Physics. 75, 733-741.

Khlebtsov, N., Trachuk, L., Mel'nikov, A., 2005. The effect of the size, shape, and structure of metal nanoparticles on the dependence of their optical properties on the refractive index of disperse medium. Optics Spectrosc. 98, 77–83.

Lenert, A., Wang, E.N., 2012. Optimization of nanofluid volumetric receivers for solar thermal energy conversion. Solar Energy. 86, 253-265.

Lenert, A., 2010. Nanofluid-based receivers for high-temperature, high-flux direct solar collectors M.Sc. Thesis. Massachusetts Institute of Technology.

Link, S., El-Sayed, M.A., 2000. Shape and size dependence of radiative, non-radiative and photothermal properties of gold nanocrystals. Int. Rev. Phys. Chem. 19, 409–423.

Maxwell, J.C., 1891. A Treatise on Electricity and Magnetism, 2 unabridged 3rd Ed., Clarendon Press. Oxford. UK.

Mercatelli, L., Sani, E., Zaccanti, G., Martelli, F., Ninni, D.P., Barison, S., Pagura, C., Agresti, F., Jafrancesco, D., 2011a. Absorption and scattering properties of carbon nanohorn-based nanofluid for direct sunlight absorbers. Nanoscale Res. Lett. 6, 282.

Mercatelli, L., Sani, E., Fontani, D., Zaccanti, G., Martelli, F., Ninni, D.P., 2011b. Scattering and absorption properties of carbon nanohorn-based nanofluids for solar energy applications. J. Euro. Optical Soc. 6, 1025.

Mercatelli, L., Sani, E., Giannini, A., Ninni, D.P., Martelli, F., Zaccanti, G., 2012. Carbon nanohorn-based nanofluids: characterization of the spectral scattering albedo. Nanoscale Research etter. 7, 96.

Minkowycz, W.J., Sparrow, E.M., Schneider, G.E., Pletcher, R.H., 1988. Hand book of numerical heat transfer. John Wiley and sons, New York.

Ovsiannikov, L.V., 1982. Group Analysis of Differential Equations. Academic Press. New York.

Sparrow, E.M., Cess, R.D., 1978. Radiation heat transfer. Hemisphere. Washington.

Rana, R., Bhargava, R., 2011. Numerical study of heat transfer enhancement in mixed convection flow along a vertical plate with heat source / sink utilizing nanofluids. Commun.Nonlinear Sci. Numer. Simulat. 16, 4318-4334.

Rosmila Abdul Kahar, Kandasamy, R., Muhaimin, I., 2011. Scaling group transformation for boundary-layer of a nanofluid past a porous vertical stretching surface in the presence of chemical reaction with heat radiation. Computers and Fluids. 52, 15-21.

Saidur, R., Leong, K.Y., Mohammad, H.A., 2011. A review on applications and challenges of nanofluids. Renew. Sustain. Energy Rev. 15, 1646–1668.

Saidur, R., Meng, T.C., Said, Z., Hasanuzzaman, M., Kamyar, A., 2012. Evaluation of the effect on nanofluid-based absorbers on direct solar collector, Int. J. Heat Mass Transfer, 55, 589–597.

Saidur, R., Kazi, S.N., Hossain, M.S., Rahman, M.M., Mohammed, H.A., 2011. A review on the performance of nanoparticles suspended with refrigerants and lubricating oils in refrigeration systems. Renew. Sustain. Energy Rev. 15, 310–323.

Sani, E., Mercatelli, L., Barison, S., Pagura, C., Agresti, F., Colla, L., Sansoni, P., 2011.
Potential of carbon nanohorn-based suspensions for solar thermal collectors. Solar Energy Mater. and Solar Cells. 95, 2994–3000.

Schlichting, H., 1979. Boundary Layer Theory. McGraw Hill Inc. New York.

Thomas, S., Sobhan, C., 2011. A review of experimental investigations on thermal phenomena in nanofluids. Nanoscale Res. Lett. 6, 377.

Vajravelu, K., Prasad, K.V., Jinho Lee, Changhoon Lee, Pop, I., Robert A. Van Gorder, 2011.Convective heat transfer in the flow of viscous Ag-water and cu-water nanofluids over a stretching surface. Int. J. of Thermal Sciences., 50, 843-851.

White, F.M., 2006. Viscous Fluid Flows. (third ed.)McGraw-Hill, New York.

Nomenclature

B_0	Magnetic field strength,
C	Nanoparticles volume fraction,
C_w	Nanoparticle volume fraction at the wall,
C_∞	Ambient nanoparticle volume fraction,
c_p	Specific heat at constant pressure,
C_T	Temperature ratio
Ec	Eckert number,
f	Dimensionless stream function,
F	Empirical constant in the second-order resistance,
F_n	Forchheimer number,
g	Acceleration due to gravity,
k	Thermal conductive,
k^*	Mean absorption coefficient
K	Permeability of the porous medium,
M	Magnetic parameter,

N	Conductive radiation parameter
n	Thermal stratification parameter
Pr_f	Prandtl number,
q''_{rad}	Incident radiation flux of intensity
S	Suction / Injection parameter
T	Temperature of the fluid,
T_w	Temperature at the wall,
T_∞	Ambient temperature,
u, v	Velocity components along x- and y- axes,
$U(x)$	Uniform velocity of the free stream flow,
v_0	Velocity of suction / injection,

Greek symbols

α_{f_n}	Thermal diffusivity of the nanofluid
β	Coefficient of thermal expansion,
θ	Dimensionless temperature,
ϕ	Dimensionless nanoparticle volume fraction,
η	Similarity variable,
μ	Dynamic viscosity,
μ_{f_n}	Effective dynamic viscosity of the nanofluid,
σ	Electric conductivity of the fluid,
σ_1	Stefan–Boltzman constant,
ρ_f	Density of the base fluid,
ρ_{f_n}	Effective density of the nanofluid,
$(\rho c)_f$	Heat capacity of the base fluid,
$(\rho c)_P$	Effective heat capacity of the nanoparticle material,
ν	Kinematic viscosity,
ψ	Stream function.
σ_1	Stefan–Boltzman constant is,
Ω	Angle of the wedge,

The IISTE is a pioneer in the Open-Access hosting service and academic event management. The aim of the firm is Accelerating Global Knowledge Sharing.

More information about the firm can be found on the homepage:
http://www.iiste.org

CALL FOR JOURNAL PAPERS

There are more than 30 peer-reviewed academic journals hosted under the hosting platform.

Prospective authors of journals can find the submission instruction on the following page: http://www.iiste.org/journals/ All the journals articles are available online to the readers all over the world without financial, legal, or technical barriers other than those inseparable from gaining access to the internet itself. Paper version of the journals is also available upon request of readers and authors.

MORE RESOURCES

Book publication information: http://www.iiste.org/book/

Academic conference: http://www.iiste.org/conference/upcoming-conferences-call-for-paper/

IISTE Knowledge Sharing Partners

EBSCO, Index Copernicus, Ulrich's Periodicals Directory, JournalTOCS, PKP Open Archives Harvester, Bielefeld Academic Search Engine, Elektronische Zeitschriftenbibliothek EZB, Open J-Gate, OCLC WorldCat, Universe Digtial Library , NewJour, Google Scholar